

NMR IMAGING OF SOLIDS WITH A SURFACE COIL

J. B. Miller and A. N. Garroway

Chemistry Division, Code 6120
Naval Research Laboratory
Washington, D.C. 20375-5000

INTRODUCTION

Nuclear magnetic resonance (NMR) imaging [1] usually exploits the dependence of the resonance frequency (generally in the rf band) on the magnetic field strength to map spatial position onto a frequency spectrum. The magnetic field strength is given a known spatial dependence and the spins are uniformly excited with an rf field. The uniform rf field is generally produced inside a cylindrical rf coil.

The rf field strength is required to be much larger than the resonance frequency linewidth of the nuclei being observed. In liquid samples the linewidth may be only a few hertz; however in solids the linewidth can be tens of kilohertz due to dipolar and chemical shift interactions which are averaged out by the molecular motions in liquids.

Generating the large rf field required for solid samples throughout a large volume can prove prohibitive in terms of transmitter output power. An alternative is to use a surface coil to generate a large rf field in a small region of the object being imaged. A common surface coil design employs a single loop or flat spiral of wire as shown in fig. 1. With a surface coil many small regions of the object can be imaged separately and pieced together to form a composite image.

A difficulty with surface coils is that they do not produce a uniform rf field throughout the region being imaged. In the work described here we use this spatial dependence of the rf field to obtain our image, keeping the magnetic field strength constant over the sample.

ROTATING FRAME IMAGING

There are a number of possible methods which use the spatial dependence of the rf field to obtain an image. A conceptually simple technique is referred to as rotating frame imaging [2,3] in the literature. In rotating frame imaging, spatial positions are mapped onto a frequency spectrum as in the normal (laboratory frame) imaging techniques. Instead of observing spatially dependent resonance frequencies however, we now observe the spatially dependent nutation

frequencies of the spins about the rf field. An example of one-dimensional rotating frame imaging of a solid is shown in fig. 2.

The object being imaged consisted of three disks of the plastic crystal adamantane separated by NMR transparent spacers, and is shown in fig. 1. The spacers were 2 mm thick and the adamantane disks were 6.5 mm in diameter and 2, 1.5, and 1 mm thick in order of increasing distance from the surface coil. The image of fig. 2 was obtained by rapidly pulsing the rf field and observing the nuclear signal, in this case from the ^1H nuclei, between pulses. The nutation signal was Fourier transformed as a function of the number of applied rf pulses to obtain the one-dimensional image.

The three disks of adamantane can be clearly seen in fig. 2, although they are not completely resolved. The spatial scale is not linear here because the rf field gradient from the surface coil is not linear.

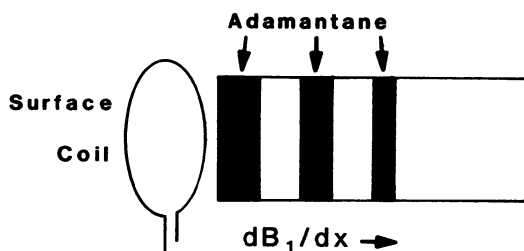


Fig. 1. The surface coil generates a rf field gradient perpendicular to the plane of the coil. The actual coil used in the experiments consisted of four concentric loops with an outer diameter of 27 mm and an inner diameter of 10 mm. The sample consisted of three disks of adamantane (shown in black) 2.0, 1.5, and 1.0 mm thick separated by 2 mm thick NMR transparent spacers.

As in laboratory frame imaging, the spatial resolution of rotating frame imaging is limited by the NMR linewidth. As in the present case, when observing high concentrations of nuclei in the laboratory frame, homonuclear dipolar couplings are generally the dominant line broadening mechanism, with additional contributions from chemical shift and heteronuclear dipolar couplings. In the rotating frame (on resonance) chemical shift and heteronuclear dipolar couplings do not contribute to the linewidth and the magnitude of homonuclear dipolar broadening is reduced by a factor of two [4]. Even so, this results in poor spatial resolution, approximately 2 mm, for the image in fig. 2. Clearly, a technique which provides higher spatial resolution is needed.

SELECTIVE EXCITATION AND DETECTION

Another possibility is to selectively excite and/or detect signals from a small area of the region to be imaged. In this way each region

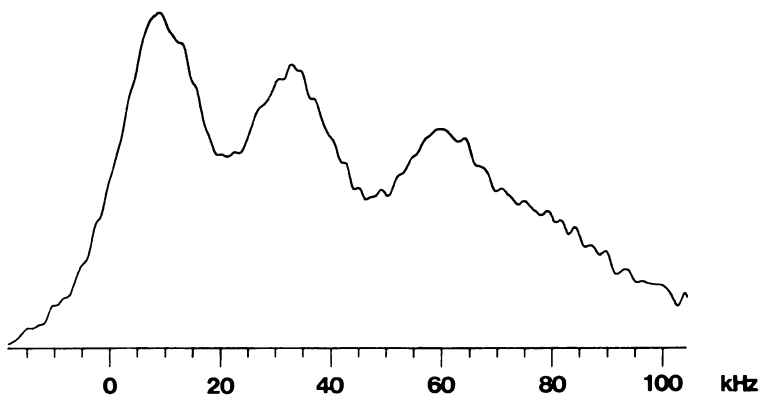


Fig. 2. One-dimensional rotating frame image of the sample shown in fig. 1. The spatial resolution near the surface coil (left side of figure) is approximately 2 mm.

of the object may be imaged point by point and the image of the entire object obtained by combining the images of the separate regions. These techniques are frequently referred to as sensitive plane or depth pulse techniques in the surface coil imaging literature [5,6].

The ideal situation would be to excite selectively the spins in a small area, leaving the surrounding spins unperturbed. This results in rapid data collection since we do not have to wait for longitudinal spin relaxation before collecting data from neighboring areas. The line broadening which interferes with NMR imaging of solids also interferes with the standard selective excitation techniques. We have chosen to address the simpler problem of selective detection.

If an rf pulse of arbitrary tip angle is applied to the spin system, the spins will be nutated away from their equilibrium position along the magnetic field. In solids, the homonuclear dipolar interaction will cause the nuclear magnetization to dephase rapidly, leaving only its projection along the magnetic field. If the rf pulse is applied with a surface coil, then the nutation angle will vary in space. In regions where the tip angle is an integral multiple of π , the full nuclear magnetization will be preserved. Elsewhere, the magnitude of the nuclear magnetization will vary as $\cos[\theta(x)]$, where $\theta(x)$ is the rf tip angle at position x . After a dephasing delay the magnetization remaining along the magnetic field can be detected. This provides a mechanism for selective detection, although the $\cos\theta$ profile is not very sharp [7]. We can appreciably sharpen the profile of the selected region by applying a series of pulses with dephasing delays between each. The resultant profile will have a $\cos^n[\theta(x)]$ dependence, where n is the number of applied pulses.

Figure 3 is a one-dimensional image of the sample shown in fig. 1. The data were obtained with the technique described above using 16 θ pulses. MREV-8 [8,9] multiple pulse line narrowing [10] was used to enhance the sensitivity during detection. The imaging dimension was scanned by stepping the transmitter output power in 0.5 dB increments.

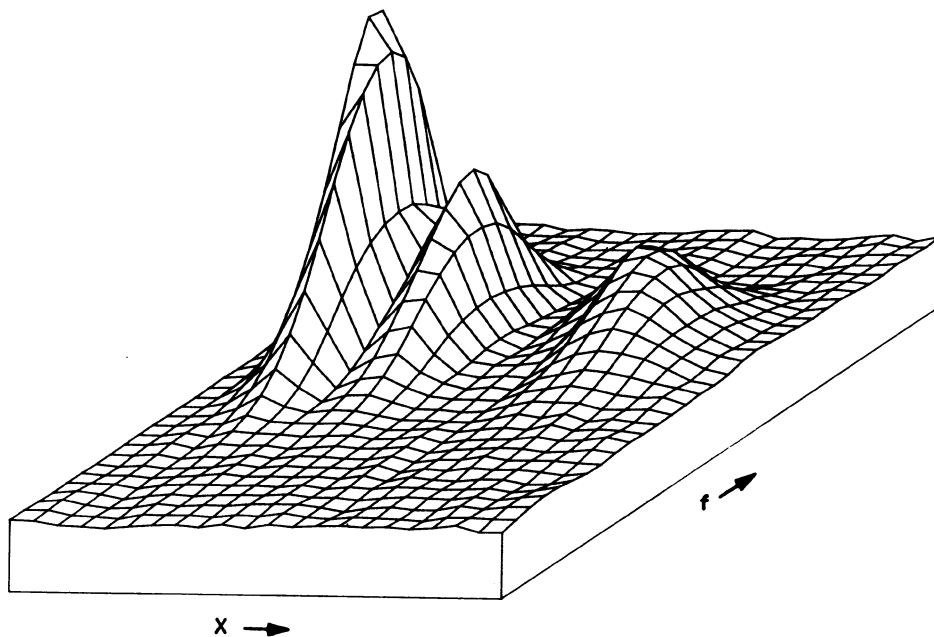


Fig. 3. One-dimensional selective detection image of the sample shown in fig. 1. The spatial dimension was obtained by stepping the transmitter power in 0.5 dB increments with 22 regions detected. Multiple pulse line narrowing was used during detection. Features smaller than 1 mm can be resolved with this technique. The spatial scale is not linear due to the nonlinearity of the rf field gradient and the nonlinear steps in transmitter power.

Now, in fig. 3, the three disks of adamantane are clearly resolved. As in fig. 2 the spatial scale is not linear. In the present case we have two causes of nonlinearity: the nonlinear rf field gradient and the nonlinear steps in transmitter power.

The selective detection scheme described above greatly improves the spatial resolution of surface coil images, but at a price. Just as with rotating frame imaging, the homonuclear dipolar interaction causes the spins to dephase as they are nutated by the rf field. Thus, at the end of the excitation pulse train only a fraction of the nuclear magnetization remains from the region to be detected. This fraction is inversely proportional to the exponent of the product of the total length of rf irradiation and the dipolar linewidth and thus can be quite small. We can improve the situation somewhat by using a more efficient pulse train (fewer pulses) to excite the spin system. Such a pulse sequence was proposed by Shaka and Freeman [11] and employs a pulse train $(\theta - d - 2\theta - d - \dots - n\theta - d -)_2$, where θ is the nominal rf nutation angle and d is the dephasing delay. (For simplicity of discussion we will consider an $n\theta$ pulse as a θ pulse repeated n times without the dephasing delays.) The subscript 2 denotes that the pulse train is repeated twice. For $n=4$, 20 θ pulses, the region selected by the Shaka and Freeman pulse sequence is twenty percent narrower than the region selected with a train of 20 identical pulses.

Even with improved pulse trains the sensitivity of selective detection can be quite poor. Further gain can be made by decoupling the homonuclear dipolar interaction during the rf pulses in a manner similar to the detection scheme we used in fig. 3. One particularly useful method we refer to as a dipolar decoupled composite inversion pulse (DDCIP) [12]. The DDCIP is composed of 6 phase-shifted rf pulses. When the individual rf pulses have a nutation angle of $\pi/2$, homonuclear dipolar dephasing will be suppressed and the net nutation angle will be π .

The effectiveness of the DDCIP is demonstrated in fig. 4. The remaining nuclear magnetization was measured after excitation with the Shaka and Freeman pulse sequence using either a simple rf pulse or the DDCIP. Measurements were made on a sample of polyacrylic with 2, 6, 12, and 20 pulses corresponding to $n=1, 2, 3,$ or 4 in the pulse train diagrammed above. For $n=4$, the DDCIP results in an order of magnitude increase in sensitivity.

Figure 5 is a one-dimensional image of a polyacrylic sample obtained with the DDCIP used in the pulse train of Shaka and Freeman.

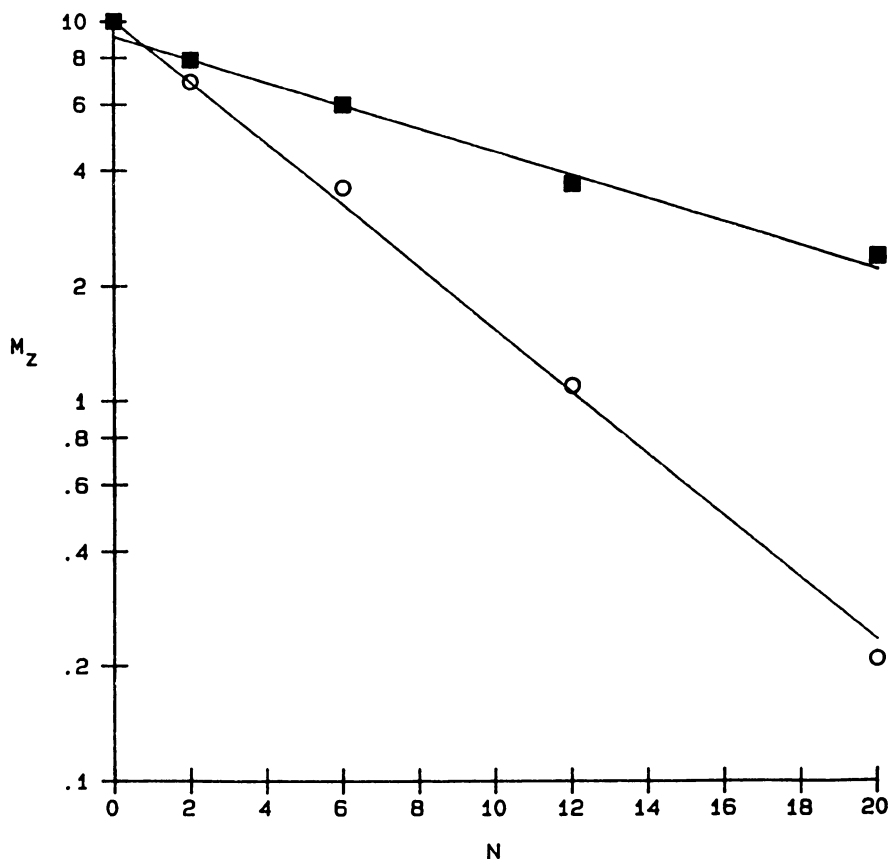


Fig. 4. Comparison of simple rf pulses and dipolar decoupled composite inversion pulses (DDCIP) using the Shaka and Freeman pulse train described in the text. At $n=4$, equivalent to 20 inversion pulses, the DDCIP (■) sequence provides an order of magnitude improvement in sensitivity over simple rf pulses (○).

The sample geometry is shown as an inset to the figure. The x dimension was obtained by stepping the transmitter power in 0.1 dB increments and the f dimension is the Fourier transform of the pulsed spin-lock signal which was used during detection to increase sensitivity. Again, the spatial dimension is nonlinear for the reasons previously given for the image in fig. 3. Near the surface coil (left side of figure) the spatial resolution is approximately 200 μm .

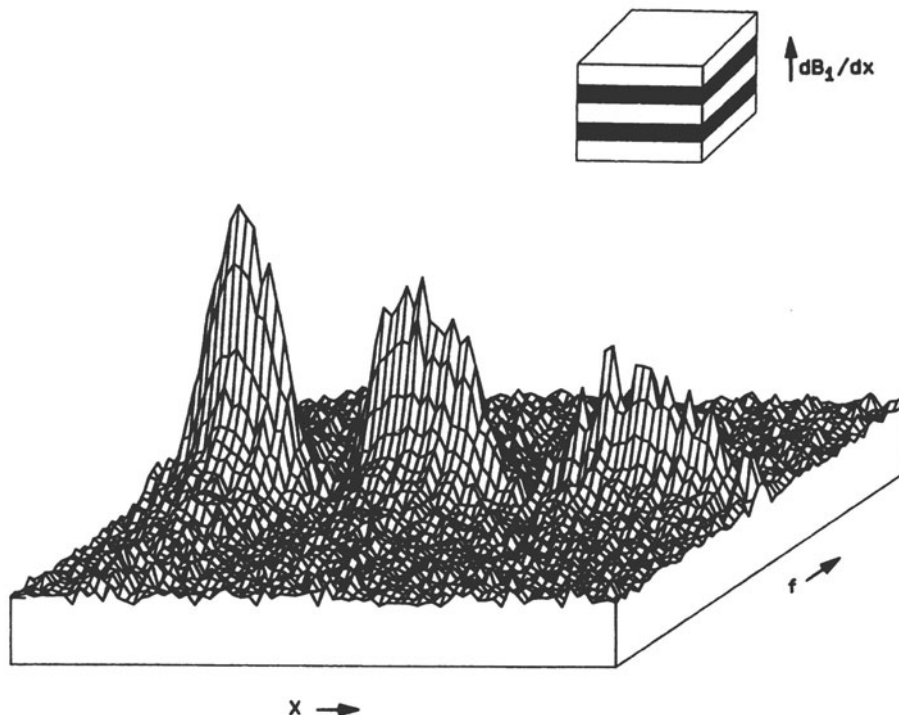


Fig. 5. One-dimensional image of the polyacrylic sample shown in the inset. The sample dimensions were 8 by 8 by 1.2 mm thick with 1 mm thick NMR transparent spacers (black regions). The image was obtained with the DDCIP by stepping the transmitter power in 0.1 dB increments with 22 regions detected. The spatial resolution is approximately 200 μm .

CONCLUSIONS

We have demonstrated techniques for NMR imaging of solids with a surface coil. The use of a surface coil for NMR imaging allows imaging of solids with modest transmitter power by concentrating the rf field in a small region of the object. The use of dipolar decoupled composite inversion pulses allows us to retain enough sensitivity to image rigid polymers such as polyacrylic.

REFERENCES

1. P. Mansfield and P. C. Morris, "Advances in Magnetic Resonance," Supp. 2, NMR Imaging in Biomedicine, (Academic Press, New York, 1982).
2. D. I. Hoult, *J. Magn. Reson.* 33, 183 (1979).
3. A. A. Maudsley, *Magn. Reson. Med.* 3, 768 (1986).
4. C. P. Slichter, Principles of Magnetic Resonance, 2nd. ed., Springer-Verlag, New York (1980).
5. M. R. Bendall and R. E. Gordon, *J. Magn. Reson.* 53, 365 (1983).
6. M. Garwood, T. Schleich, B. D. Ross, G. B. Matson, and W. D. Winters, *J. Magn. Reson.* 65, 239 (1985).
7. J. B. Miller and A. N. Garroway, *J. Magn. Reson.* 77, 187 (1988).
8. P. Mansfield, *J. Phys. C* 4, 1444 (1971).
9. (a) W. -K. Rhim, D. D. Elleman, and R. W. Vaughan, *J. Chem. Phys.* 58, 1772 (1973); (b) W. -K. Rhim, D. D. Elleman, and R. W. Vaughan, *J. Chem. Phys.* 59, 3740 (1973).
10. M. Mehring, "NMR-Basic Principles and Progress," Vol. 11, High Resolution NMR in Solids, 2nd ed., (Springer-Verlag, New York, 1983).
11. A. J. Shaka and R. Freeman, *J. Magn. Reson.* 64, 145 (1985).
12. J. B. Miller and A. N. Garroway, *J. Magn. Reson.*, in press.